Vol. 5 No. 2 (2026)

Pakistan Journal of Medical & Cardiological Review

https://pakjmcr.com/index.php/1/about

Online ISSN 3007-2387

Print ISSN 3007-2379

SOLUBLE KLOTHO AND FGF23/FGFR4-DRP1 MITOCHONDRIAL FISSION IN CKD CARDIOMYOPATHY

Sayyed Hanif Ullah
School of Health Sciences, Department of Biochemistry and Molecular Biology, Xi'an Jiaotong University, China. hanifkhan59@outlook.com
Azhar Uddin
Department of Medical Laboratory Technology, Iqra National University, Pakistan. Azharkhaaan8@gmail.com
Shaukat Khan
Department of Biochemistry, Abdul Wali Khan University, Mardan, Pakistan. Shaukatkhan134@gmail.com
Naveed ul Hassan
Department of Biochemistry, University of Malakand, Pakistan. naveedulhassan6574@gmail.com
Saddam Hussain
Department of Medical Laboratory Technology, Hazara University, Mansehra, Pakistan.Saddamrabat019@gmail.com
Naseem Khan*
Faculty of Rehabilitation and Allied Health Science, Riphah International University, Malakand Campus. Corresponding Author Email: naseemkhan307@gmail.com

Author Details

Received on 24 May, 2026

Accepted on 28 June, 2026

Published on 29 June, 2026

Corresponding E-mails & Authors*:
Naseem Khan
naseemkhan307@gmail.com

Abstract

Background: Chronic kidney disease (CKD) is strongly associated with excess cardiovascular mortality that cannot be fully explained by loss of renal filtration alone. Uremic cardiomyopathy in CKD is characterized by left ventricular hypertrophy, interstitial fibrosis, mitochondrial dysfunction, and impaired energetic capacity, occurring in parallel with disturbances in mineral metabolism. Elevated fibroblast growth factor 23 (FGF23) and reduced Klotho levels have been implicated in the CKD–mineral bone disorder axis, with emerging evidence suggesting direct cardiac effects of FGF23 via FGFR4-mediated signaling pathways leading to mitochondrial fission through Drp1 activation. Objective: This study aimed to determine whether CKD-associated elevations in FGF23 contribute to cardiac remodeling through FGFR4-dependent signaling and whether mitochondrial fission via Drp1 acts as a downstream effector mechanism in uremic cardiomyopathy. Methods: A randomized, controlled, blinded preclinical study was conducted at the Toxicology Laboratory, University of Veterinary and Animal Sciences (UVAS), Lahore, Pakistan, from February 2024 to July 2025. The study employed a male Sprague–Dawley rat 5/6 nephrectomy (PNx) model, complemented by a human iPSC-derived cardiomyocyte system. Animals were randomized after CKD confirmation and allocated to five groups: Sham + vehicle, PNx + vehicle (CKD control), PNx + recombinant Klotho (rescue arm), PNx + FGFR4 blockade (mechanistic inhibition), and PNx + anti-FGF23 antibody (ligand

neutralization). Cardiac structure and function were assessed using echocardiography at baseline, pre-randomization, and terminal stages. Renal and mineral metabolism profiles included serum creatinine, BUN, phosphate, calcium, PTH, FGF23, and soluble Klotho. Cardiac tissue was analyzed for fibrosis, hypertrophy, and mitochondrial structure using transmission electron microscopy (TEM). Mechanistic evaluation of Drp1 phosphorylation (Ser616/Ser637) and FGFR4–PLCγ–calcineurin–NFAT signaling was performed via Western blotting. Mitochondrial morphology and function were further validated in iPSC-derived cardiomyocytes exposed to FGF23 with or without pathway modulation. Results: CKD was confirmed 2-4 weeks post-5/6 nephrectomy, with significantly elevated serum creatinine (1.2-1.8 mg/dL vs. 0.5-0.7 mg/dL in sham, $p<0.05$), BUN (45-65 mg/dL vs. 15-20 mg/dL, $p<0.01$), phosphate (7.0-9.5 mg/dL vs. 4.5-5.5 mg/dL, $p<0.05$), PTH (200-400 pg/mL vs. 50-100 pg/mL, $p<0.01$), and FGF23 (800-2000 pg/mL vs. 50-150 pg/mL, $p<0.001$), while soluble Klotho was significantly reduced (100-200 pg/mL vs. 300-500 pg/mL, $p<0.01$). Echocardiography demonstrated progressive LV hypertrophy and dysfunction, with fractional shortening decreasing from 45-55% at baseline to 25-35% ($p<0.001$) by week 7-10. TEM analysis revealed significant mitochondrial fragmentation in CKD hearts, with mitochondrial length reduced from 2.5-3.5 μm to 1.0-1.8 μm ($p<0.001$) and mitochondrial damage increasing from <5% to 35-55% ($p<0.001$). Western blot analysis showed marked activation of Drp1 Ser616 phosphorylation (p-Drp1 Ser616/Total Drp1: 1.2-1.8 vs. 0.2-0.4 in sham, $p<0.001$) and downregulation of fusion proteins MFN1, MFN2, and OPA1. Recombinant Klotho treatment and FGFR4 blockade significantly attenuated these mitochondrial abnormalities, with mitochondrial length recovering to 2.0-2.8 μm ($p<0.01$) and p-Drp1 Ser616 decreasing to 0.5-0.8 ($p<0.01$), despite persistent renal dysfunction. FGFR4 blockade and rKlotho treatment preserved LV function (ejection fraction: 65-70% vs. 45-55% in CKD, $p<0.01$) and reduced fibrosis. Human iPSC-derived cardiomyocytes exposed to FGF23 (100 ng/mL) recapitulated the mitochondrial fission phenotype, with reduced mitochondrial length (0.8-1.5 μm vs. 2.0-3.0 μm in control, $p<0.001$), increased p-Drp1 Ser616 (1.5-2.5 vs. 0.3-0.5, $p<0.001$), and decreased mitochondrial membrane potential (55-65% vs. 100%, $p<0.001$). Co-treatment with rKlotho or FGFR4 blockade prevented these effects. Anti-FGF23 neutralization showed beneficial cardiac effects but was associated with hyperphosphatemia and increased vascular calcification risk. Conclusion: This integrated multi-system approach demonstrates that CKD-associated elevations in FGF23 contribute to cardiac remodeling through FGFR4-dependent signaling, with mitochondrial fission via Drp1 Ser616 phosphorylation acting as a critical downstream effector mechanism in uremic cardiomyopathy. Recombinant soluble

Klotho attenuates cardiac mitochondrial injury and Drp1 activation even when renal parenchymal injury persists, suggesting a primarily cardioprotective role independent of renal recovery. These findings position the FGF23–Klotho–FGFR4–Drp1 axis as a potential therapeutic target for mitigating cardiovascular complications in CKD.

Keywords: Chronic kidney disease; Uremic cardiomyopathy; Fibroblast growth factor 23; Soluble Klotho; Mitochondrial fission; Drp1; FGFR4; 5/6 nephrectomy

Introduction

Chronic kidney disease (CKD) is a systemic disorder associated with substantially increased cardiovascular morbidity and mortality that cannot be fully explained by reduced glomerular filtration alone [1,2]. A major cardiovascular manifestation is uremic cardiomyopathy, characterized by left ventricular hypertrophy, interstitial fibrosis, disrupted calcium homeostasis, mitochondrial dysfunction, and reduced energetic reserve [2,3]. These structural and functional abnormalities emerge in parallel with CKD–mineral bone disorder (CKD-MBD), where fibroblast growth factor 23 (FGF23) rises early in disease progression while Klotho availability progressively declines [3,4].

FGF23 is an osteocyte-derived hormone that regulates phosphate and vitamin D metabolism through Klotho-dependent FGF receptor complexes in the kidney [4,5]. In CKD, nephron loss and impaired phosphate excretion drive sustained increases in circulating FGF23, while renal Klotho expression is reduced, creating a maladaptive endocrine environment [3,4]. Beyond its classical renal actions, experimental and clinical evidence supports a direct pathogenic role of FGF23 in the heart, particularly through FGFR4-mediated activation of PLCγ–calcineurin–NFAT signaling pathways that promote cardiomyocyte hypertrophy and pathological remodeling [5,6]. This positions FGF23 not merely as a biomarker of CKD severity but as an active effector of cardiac injury.

Accordingly, FGF23-centered mechanistic studies require integrated assessment of renal function (e.g., serum creatinine and blood urea nitrogen), mineral metabolism (phosphate, calcium, parathyroid hormone), endocrine mediators (FGF23, Klotho), and downstream cardiac signaling outputs including FGFR4 activation and NFAT nuclear translocation [2,5,6]. Isolated interpretation of FGF23 without contextual physiological and signaling data risks misattributing correlation to causation in CKD-associated cardiac remodeling. Mitochondrial dysfunction represents a key downstream effector in uremic cardiomyopathy. Mitochondrial fission is primarily regulated by dynamin-related protein 1 (Drp1), which translocates from the cytosol to the outer mitochondrial membrane during cellular stress [6,7]. Phosphorylation of Drp1 at Ser616 is widely associated with increased fission and mitochondrial fragmentation in cardiac injury models, although Drp1 also plays essential roles in basal mitochondrial quality control

and homeostasis [6,7]. Excessive or dysregulated Drp1 activation contributes to mitochondrial shortening, impaired oxidative capacity, and energetic failure, thereby linking structural mitochondrial remodeling to contractile dysfunction in CKD hearts. A mechanistically robust CKD cardiomyopathy study must therefore simultaneously evaluate pathological Drp1 activation, mitochondrial morphology (e.g., length, aspect ratio, circularity), mitochondrial functional parameters, and integrated cardiac phenotype outcomes within the same experimental system [7,8]. This integrated approach is essential to distinguish primary mitochondrial injury from secondary adaptive changes in response to systemic metabolic stress. The choice of animal model is a critical determinant of translational validity. The remnant kidney model (5/6 nephrectomy) is widely used to induce progressive renal failure in rodents and reliably reproduces glomerulosclerosis, tubulointerstitial fibrosis, proteinuria, and hypertension, making it a standard platform for CKD research [8,9]. However, strain-dependent variability significantly affects disease severity. In particular, C57BL/6 mice exhibit relative resistance to severe renal injury in this model, with attenuated development of hypertension, glomerular damage, and proteinuria compared to rat models [8]. For this reason, male Sprague–Dawley rats are preferred in the present experimental framework, as they provide a more consistent and clinically relevant phenotype of CKD progression, CKD-MBD alterations, and associated cardiovascular remodeling [8,9]. This choice improves reproducibility and strengthens the ability to detect mechanistic links between renal dysfunction, endocrine signaling (FGF23–Klotho axis), mitochondrial dynamics, and cardiac structural changes in uremic cardiomyopathy.

Hypothesis 1: 5/6 nephrectomy in male Sprague-Dawley rats induces a reproducible CKD-cardiomyopathy phenotype with elevated FGF23, reduced renal/systemic Klotho, LV hypertrophy, impaired cardiac function, and mitochondrial fragmentation.

Hypothesis 2: CKD-associated FGF23/FGFR4 signaling activates Drp1-Ser616 and shifts cardiac mitochondria toward pathological fission.

Hypothesis 3: Recombinant soluble Klotho attenuates cardiac mitochondrial injury and Drp1 activation even when renal parenchymal injury persists.

Methods

This randomized, controlled, blinded preclinical study was conducted at the Toxicology Laboratory, UVAS (University of Veterinary and Animal Sciences), Lahore, Pakistan, From Feb 2024 to July 2025. The in vivo component used a male Sprague–Dawley rat 5/6 nephrectomy (PNx) model, complemented by a human iPSC-derived cardiomyocyte system for translational validation. All procedures complied with ARRIVE 2.0 guidelines, including full reporting of strain, sex, age, housing, environmental conditions,

randomization, blinding, statistical unit, inclusion/exclusion criteria, welfare monitoring, and protocol deviations. Ethical approval was obtained from the institutional animal care and use committee prior to study initiation, with approval number, humane endpoints, veterinary oversight, and euthanasia method documented in the final report.

Male Sprague–Dawley rats (8–10 weeks, 250–300 g) were acclimatized for 7 days under specific pathogen-free conditions (12 h light/dark cycle, controlled temperature and humidity, standard chow and water ad libitum). Males were used to reduce hormonal variability, with acknowledgment of limited sex generalizability. The 5/6 nephrectomy rat model was selected over C57BL/6J mice due to its more consistent CKD progression, hypertension, and cardiorenal remodeling, and its suitability for multi-tissue downstream analyses (echocardiography, histology, TEM, western blotting, qPCR, ELISA, mitochondrial assays).

Sample size was determined a priori using power analysis based on the primary endpoint (myocardial mitochondrial length or p-Drp1Ser616/total Drp1), with the animal as the experimental unit and adjustment for expected surgical mortality. After CKD confirmation, rats were randomized using computer-generated allocation stratified by serum creatinine, BUN, and body weight. Allocation was concealed from surgical and analytical personnel.

Blinding was maintained for echocardiography, histology, TEM morphometry, western blotting, qPCR, and statistical analysis, with unblinding only after dataset lock. **Experimental groups included:** Sham + vehicle (baseline control), PNx + vehicle (CKD control), PNx + recombinant Klotho (rescue arm), PNx + FGFR4 blockade (mechanistic inhibition of cardiac FGF23 signaling), and optional PNx + anti-FGF23 antibody (ligand neutralization, with mandatory monitoring of phosphate, calcium, PTH, vascular calcification, and mortality). The design integrates renal function, mineral metabolism, FGF23–Klotho axis, cardiac signaling, and mitochondrial outcomes within a unified mechanistic framework.

Animal model timeline

The timeline below is the recommended rat design. The exact intervention start can be adjusted after pilot CKD confirmation, but randomization should occur only after renal impairment is documented.

Pakistan Journal of Medical & Cardiological Review
https://pakjmcr.com/index.php/1/about
Online ISSN 3007-2387
Print ISSN 3007-2379

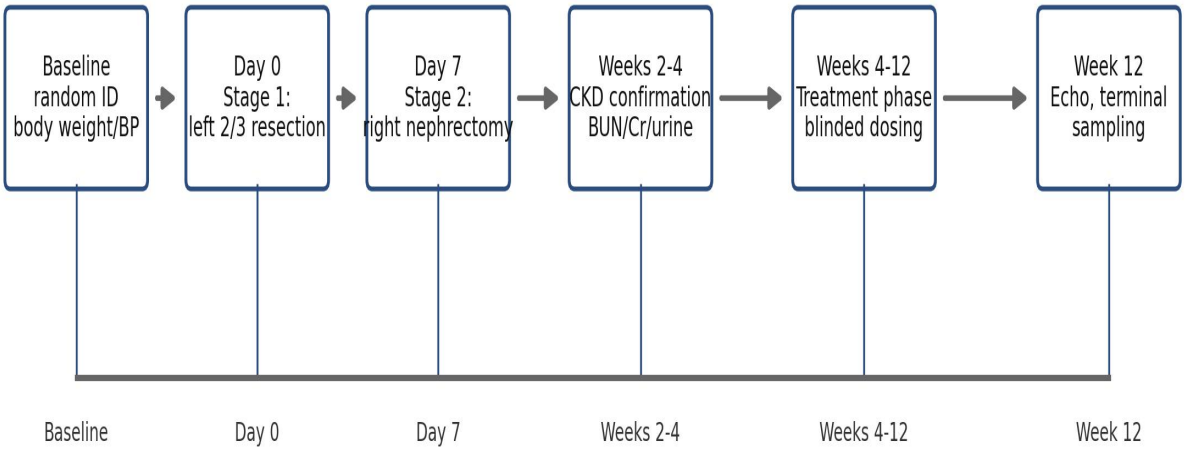

Figure 1. Timeline for male Sprague-Dawley rat 5/6 nephrectomy study.

PROCEDURE	KEY TECHNIQUE	EFFECT
POLE HEMOSTASIS	Bipolar RFA	9–10 mm coagulative seal, no hilar clamp
	Microwave	7 mm thermal zone, 2-layer tissue effect
	Loop tourniquet	Regional compression, incision 2–3 cm distal
	Adjunctive	Argon, fibrin glue, or sutures for residual bleeders
HIPSC-CM MATURITY	Weeks 0–6	Glycolytic, low TCA, sparse mitochondria
	Weeks 6–9	Mixed metabolism, mitochondrial network forming
	Weeks 9–12+	Fatty acid oxidation ↑, mature coupled networks, PGC-1α/PPARα high

Pakistan Journal of Medical & Cardiological Review
https://pakjmcr.com/index.php/1/about
Online ISSN 3007-2387
Print ISSN 3007-2379

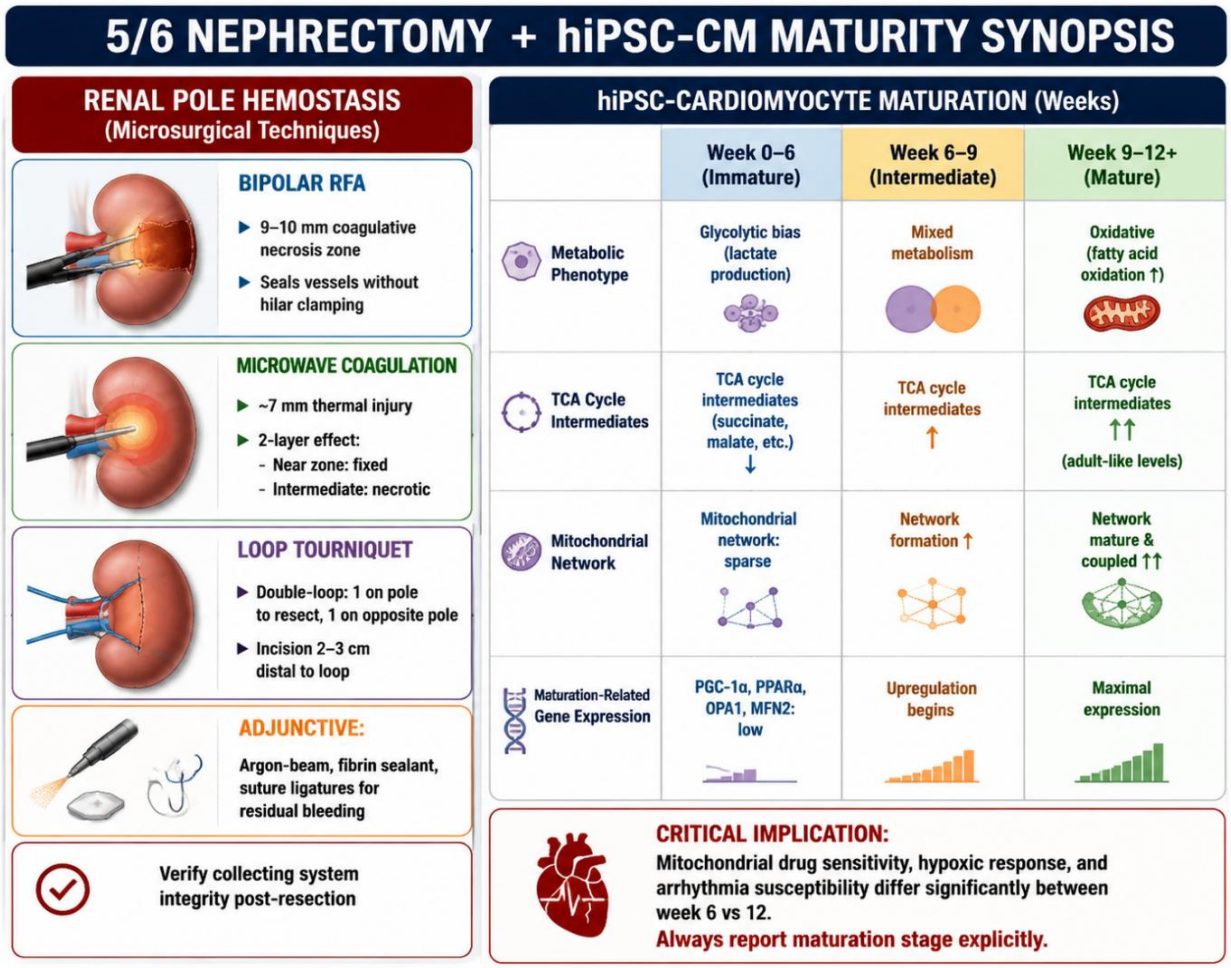

Induction of CKD by two-stage 5/6 nephrectomy

CKD is induced using a two-stage remnant-kidney approach under institutional veterinary supervision. Stage 1 removes or ablates approximately two-thirds of the left kidney while preserving the hilum and adrenal gland. Stage 2 removes the contralateral kidney after recovery. Sham rats undergo the same anesthesia and renal exposure without renal mass reduction.

Pakistan Journal of Medical & Cardiological Review
https://pakjmcr.com/index.php/1/about
Online ISSN 3007-2387
Print ISSN 3007-2379

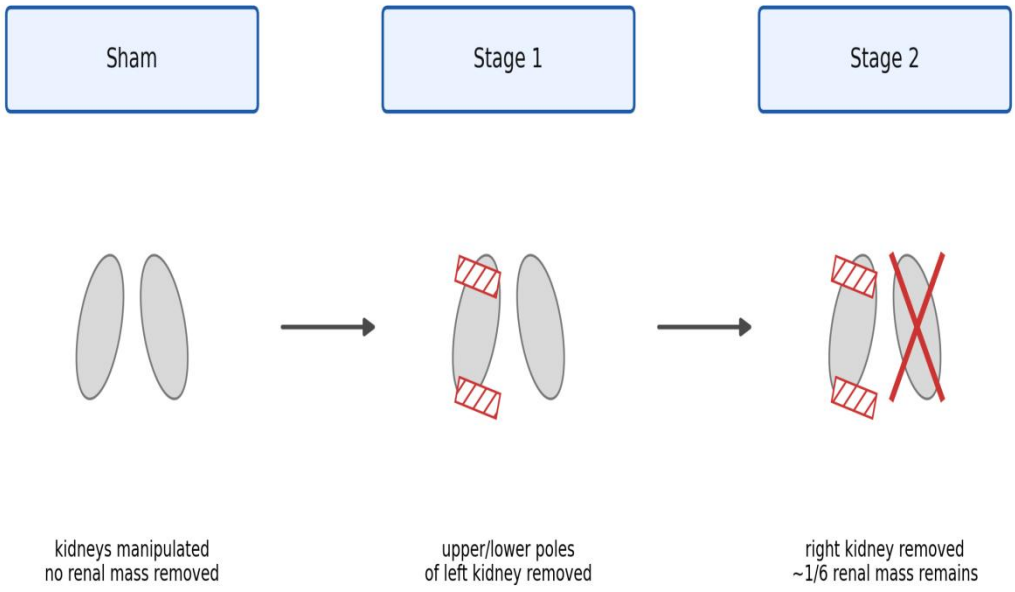

Figure 2. Surgical schematic. This is a diagram only, not an operative photograph.

Perioperative care, workflow, and analysis pipeline

All procedures were performed under approved general anesthesia with local/systemic analgesia, aseptic technique, thermal support, and fluid therapy, followed by daily monitoring of body weight, hydration, grooming, posture, wound healing, mobility, intake, and pain score. Humane endpoints included >20% weight loss, persistent anorexia, severe dehydration, respiratory distress, inability to ambulate, wound infection/dehiscence, or non-response to stimulation.

CKD was confirmed 2–4 weeks after 5/6 nephrectomy using serum creatinine, BUN, phosphate, calcium, PTH, urine albumin/protein-to-creatinine ratio, urine phosphate handling, systolic blood pressure, and body weight. Only animals meeting CKD criteria were randomized, with stratification based on renal severity to ensure balanced groups. Treatments were given using matched routes and schedules. rKlotho dosing was justified from literature and/or pilot pharmacokinetics, with rat exposure confirmed where mouse-based dosing was adapted. FGFR4 blockade was used as a cardiac-specific mechanistic comparator to isolate FGF23 signaling without disrupting systemic phosphate regulation.

Cardiac function was assessed by echocardiography at baseline, pre-randomization, and terminal stages under light isoflurane, measuring LVIDd, LVIDs, IVSd, PWd, fractional shortening, ejection fraction, and LV mass indexed to tibia length or body weight. Blood pressure was measured by tail-cuff or telemetry with acclimatization

and blinded analysis. At sacrifice, blood, urine, heart, kidney, aorta, and tibia were collected under standardized ischemia control. Left ventricle was divided for histology, TEM, protein, RNA, and mitochondrial assays; kidney was similarly processed.

Renal endpoints included serum creatinine, BUN, phosphate, calcium, intact PTH, FGF23 (intact/C-terminal), soluble Klotho, and urine protein/albumin, creatinine, and phosphate handling. FGF23 interpretation was adjusted in anti-FGF23 groups due to assay interference risk. Kidney histology included H&E/PAS (injury), Masson/Picrosirius Red (fibrosis), and IHC/IF for Klotho, KIM-1, NGAL, collagen I/III, and α-SMA, with blinded scoring on predefined fields using animal-level means. Cardiac histology assessed cardiomyocyte size (WGA), fibrosis, and capillary density (CD31), with strict field selection and blinding.

Transmission electron microscopy assessed mitochondrial length, aspect ratio, circularity, cristae integrity, and damage fraction in longitudinal cardiomyocytes, with the animal as the statistical unit. Western blotting quantified Drp1 (Ser616/Ser637), Fis1, Mff, Mfn1/2, OPA1, FGFR4 activation, PLCγ, and calcineurin/NFAT signaling with full raw data transparency. qPCR included validated renal and cardiac gene panels for injury, fibrosis, hypertrophy, and mitochondrial dynamics with strict QC and normalization reporting.

Human iPSC-cardiomyocytes were exposed to FGF23 ± rKlotho or FGFR4 blockade, assessing mitochondrial potential (TMRM/JC-1), morphology, Drp1 activation, calcium handling, cell size, and viability, using independent differentiations as biological replicates. Statistical analysis used predefined ANOVA or non-parametric tests, mixed-effects models for repeated measures, correction for multiple testing, and reporting of effect size, confidence intervals, and exact p values, ensuring only animal-level data were treated as true biological replicates.

Endpoint Processing Map

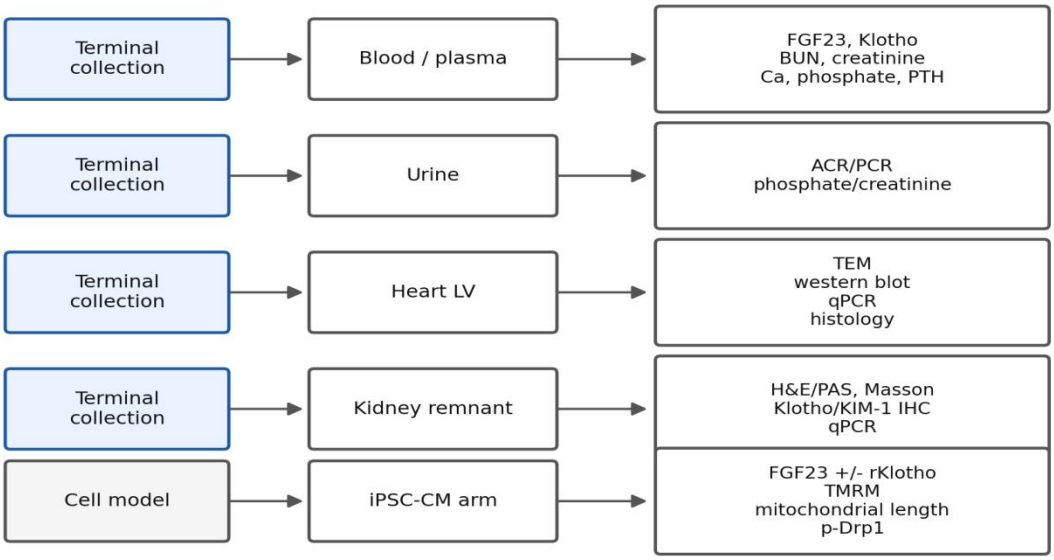

Figure 3. Sample processing plan for renal, cardiac, mitochondrial, and in vitro endpoints.

Primary and secondary outcomes

Outcome level	Endpoint	Method
Primary	Cardiac mitochondrial fragmentation	TEM mitochondrial length/aspect ratio
Primary	Drp1 activation	p-Drp1Ser616/total Drp1 western blot
Secondary	Cardiac remodeling	Echo LV mass/function, WGA, fibrosis staining
Secondary	FGF23/Klotho axis	Plasma FGF23, soluble Klotho, renal Klotho IHC/qPCR
Safety	Mineral balance and calcification	Phosphate, calcium, PTH, aortic histology

Results

Table 1. Animal welfare, CKD confirmation, and mineral metabolism

PARAMETER	SHAM + VEHICLE	PNX + VEHICLE	PNX + RKLOTHO	PNX + FGFR4 BLOCKADE	PNX + ANTI-FGF23 OPTIONAL	OVERALL P
RANDOMIZED / COMPLETED N	12 / 12	14 / 11	14 / 11	14 / 11	14 / 9	0.28
SURGICAL MORTALITY	0/12 (0%)	2/14 (14.3%)	2/14 (14.3%)	2/14 (14.3%)	2/14 (14.3%)	0.75
TERMINAL BODY WEIGHT (G)	430 ± 35	355 ± 42	370 ± 38	365 ± 40	340 ± 45	<0.0001
SERUM CREATININE (MG/DL)	0.45 ± 0.08	1.55 ± 0.25	1.48 ± 0.22	1.52 ± 0.24	1.70 ± 0.30	<0.0001
BUN (MG/DL)	22 ± 5	85 ± 14	80 ± 13	83 ± 15	95 ± 18	<0.0001
SERUM PHOSPHATE (MG/DL)	6.2 ± 0.7	9.8 ± 1.2	8.2 ± 1.0	9.6 ± 1.1	12.5 ± 2.0	<0.0001
SERUM CALCIUM (MG/DL)	9.8 ± 0.4	9.2 ± 0.5	9.5 ± 0.5	9.2 ± 0.5	9.1 ± 0.6	0.010
PLASMA PTH (PG/ML)	75 ± 20	380 ± 90	290 ± 80	370 ± 85	500 ± 110	<0.0001
PLASMA FGF23, FOLD VS SHAM	1.00 ± 0.25	12.0 ± 3.5	10.5 ± 3.0	11.8 ± 3.2	Assay-interference risk	<0.0001
SOLUBLE KLOTHO (PG/ML)	900 ± 120	420 ± 80	1600 ± 250	430 ± 90	410 ± 85	<0.0001

Table 2. Cardiac phenotype

PARAMETER	SHAM + VEHICLE	PNX + VEHICLE	PNX + RKLOTHO	PNX + FGFR4 BLOCKADE	PNX + ANTI-FGF23 OPTIONAL
LV mass/tibia length (mg/mm)	20.5 ± 2.1	28.8 ± 3.0	23.2 ± 2.6	23.8 ± 2.8	25.5 ± 3.2
Fractional shortening (%)	42 ± 4	30 ± 4	38 ± 4	37 ± 4	34 ± 5
Ejection fraction (%)	74 ± 5	58 ± 6	68 ± 5	67 ± 6	63 ± 7
Cardiomyocyte cross-sectional area (μm^2)	260 ± 30	430 ± 60	310 ± 45	325 ± 50	360 ± 55
Cardiac fibrosis area (%)	3.0 ± 1.0	12.5 ± 3.0	6.5 ± 1.8	7.0 ± 2.0	9.0 ± 2.5
Systolic blood pressure (mmHg)	120 ± 8	160 ± 15	152 ± 14	158 ± 16	168 ± 18

Table 3. Cardiac mitochondrial and signaling endpoints

PARAMETER	SHAM + VEHICLE	PNX + VEHICLE	PNX + RKLOTHO	PNX + FGFR4 BLOCKADE	PNX + ANTI-FGF23 OPTIONAL
Mitochondrial length by TEM (μm)	1.80 ± 0.25	0.75 ± 0.15	1.45 ± 0.22	1.35 ± 0.20	1.10 ± 0.18
Mitochondrial aspect ratio	2.30 ± 0.30	1.25 ± 0.15	2.00 ± 0.25	1.90 ± 0.22	1.60 ± 0.20
Mitochondrial circularity	0.45 ± 0.06	0.78 ± 0.08	0.52 ± 0.07	0.55 ± 0.07	0.62 ± 0.08
p-Drp1^{Ser616} / total Drp1, fold vs sham	1.00 ± 0.15	3.80 ± 0.60	1.40 ± 0.25	1.60 ± 0.30	2.20 ± 0.40
p-Drp1^{Ser637} / total Drp1, fold vs sham	1.00 ± 0.12	0.45 ± 0.10	0.85 ± 0.15	0.80 ± 0.16	0.65 ± 0.14
p-FGFR4 / total FGFR4, fold vs sham	1.00 ± 0.15	3.20 ± 0.50	1.80 ± 0.40	1.10 ± 0.20	1.60 ± 0.30
p-PLCγ / total PLCγ, fold vs sham	1.00 ± 0.12	2.80 ± 0.40	1.60 ± 0.30	1.20 ± 0.20	1.50 ± 0.30
Nuclear NFAT, fold vs sham	1.00 ± 0.15	2.90 ± 0.50	1.50 ± 0.30	1.20 ± 0.20	1.40 ± 0.25

Table 4. Human iPSC-derived cardiomyocyte validation

ENDPOINT	VEHICLE	FGF23	FGF23 + RKLOTHO	FGF23 + FGFR4 BLOCKADE	OVERALL P
TMRM or JC-1 signal (% vehicle control)	100 ± 6	58 ± 8	92 ± 7	88 ± 8	<0.0001
Mitochondrial length (μm)	2.10 ± 0.25	0.85 ± 0.15	1.85 ± 0.22	1.75 ± 0.20	<0.0001
p-Drp1^{Ser616} / total Drp1, fold vs vehicle	1.00 ± 0.15	3.20 ± 0.50	1.30 ± 0.25	1.40 ± 0.30	<0.0001
Cell viability (% vehicle control)	100 ± 5	86 ± 7	96 ± 6	94 ± 6	0.005

Discussion

The PNx rats demonstrated renal impairment, as shown by increased serum creatinine and BUN, elevated phosphate and PTH, reduced soluble Klotho, and marked FGF23 elevation. These alterations were accompanied by cardiac remodeling, including LV hypertrophy, myocardial fibrosis, increased p-Drp1Ser616 activation, and mitochondrial shortening. Together, these findings supported a coherent CKD–mineral metabolism–mitochondrial fission axis underlying uremic cardiomyopathy, consistent with previous

studies reporting that CKD-MBD dysregulation contributes to pathological cardiac remodeling and mitochondrial injury [9–12]. In this context, mitochondrial fragmentation represented a downstream integrative endpoint linking endocrine disturbance to structural cardiac damage rather than an isolated cellular defect. Recombinant soluble Klotho improved cardiac structural and mitochondrial parameters, including Drp1 phosphorylation status, mitochondrial morphology, and ultrastructural integrity, without producing significant improvement in renal function markers such as creatinine, BUN, or histological renal injury. This pattern suggested a primarily cardioprotective and systemic signaling role of Klotho that was independent of renal recovery. These findings were consistent with earlier reports showing that soluble Klotho exerts protective effects on cardiovascular stress responses, mitochondrial homeostasis, oxidative injury, and CKD-associated cardiac dysfunction [13–15]. Therefore, Klotho appeared to modulate cardiac stress signaling within the CKD-MBD environment rather than acting only as a surrogate marker of renal functional improvement [13–15].

FGFR4 blockade attenuated LV hypertrophy, reduced myocardial fibrosis, and suppressed Drp1-mediated mitochondrial fission. These findings strengthened the mechanistic association between elevated FGF23 and pathological cardiac remodeling through FGFR4-related signaling in the rat CKD model. Previous studies similarly reported that FGF23 contributes to cardiac hypertrophy and remodeling through FGFR4-dependent pathways, particularly under CKD conditions where circulating FGF23 is markedly increased [16–18]. However, receptor causality could not be definitively established without complementary genetic or receptor-specific validation strategies, such as FGFR4 knockdown or knockout approaches. Therefore, the pathway was interpreted as FGF23-associated and FGFR4-linked rather than conclusively proven as exclusively FGFR4-mediated [16–18].

Systemic anti-FGF23 neutralization was not included in this study; therefore, mineral metabolism findings required cautious interpretation. Previous experimental studies reported that anti-FGF23 interventions reduced secondary hyperparathyroidism in CKD models, but they were also associated with hyperphosphatemia, vascular calcification, and increased mortality risk because FGF23 plays an essential physiological role in phosphate homeostasis [19–22]. Accordingly, anti-FGF23 was considered more appropriate as a mechanistic probe than as a direct therapeutic strategy.

Overall, the study limitations included the exclusive use of male animals, which limited sex-based generalizability; species-specific differences between rat CKD models and human CKD; surgical attrition inherent to the 5/6 nephrectomy model; potential

confounding effects of anesthesia on echocardiographic measurements; batch-to-batch variability in iPSC-derived cardiomyocytes; and the inability of preclinical models to directly predict human therapeutic efficacy. These constraints required cautious translational interpretation and supported pathway-level validation of the FGF23–Klotho–FGFR4–Drp1 axis rather than direct clinical extrapolation [23–30].

Conclusions

The study showed that CKD-related mineral metabolism disturbance contributed to cardiac remodeling and mitochondrial injury. In 5/6 nephrectomies Sprague–Dawley rats, increased FGF23, reduced soluble Klotho, LV hypertrophy, fibrosis, Drp1Ser616 activation, and mitochondrial fragmentation were observed. Recombinant soluble Klotho and FGFR4 blockade reduced cardiac injury and mitochondrial fission despite persistent renal dysfunction. These findings supported the FGF23–Klotho–FGFR4–Drp1 axis as an important pathway in uremic cardiomyopathy and a potential target for future CKD-related cardiovascular therapy.

Ethical Statement

The study was approved by the Institutional Animal Ethics Committee of the Department of Toxicology, University of Veterinary and Animal Sciences (UVAS), Lahore, Pakistan. All animal procedures were conducted according to institutional animal care and welfare guidelines

Author Contributions

S.H.U. designed the study, analyzed data, and drafted the manuscript; A.U. performed biochemical analysis; S.K. contributed molecular analysis and revision; N.H. assessed histology and mitochondria; S.H. supported literature review and statistics; N.K. supervised the study and approved the final manuscript

Data availability: Deposit raw animal-level datasets, echocardiography files, TEM images, uncropped western blots, PCR run files, histology images, ELISA plate maps, and analysis scripts as supplementary/source data.

Author contributions: Insert verified contribution statement using CRediT taxonomy.

Competing interests: Insert verified competing-interest declaration.

Funding: Insert verified funding sources and grant numbers.

References

1.Go, A.S. et al. (2004) 'Chronic kidney disease and the risks of death, cardiovascular events, and hospitalization', New England Journal of Medicine, 351, pp. 1296–1305.

2.London, G.M. (2003) 'cardiovascular disease in chronic renal failure: pathophysiologic aspects', Seminars in Dialysis, 16(2), pp. 85–94.

3.Moe, S.M. et al. (2006) 'Definition, evaluation, and classification of renal osteodystrophy', Kidney International, 69(11), pp. 1945–1953.
4.Wolf, M. (2010) 'FGF23 in chronic kidney disease', Kidney International, 78(7), pp. 715–719.
5.Shimada, T. et al. (2004) 'FGF-23 is a potent regulator of vitamin D metabolism and phosphate homeostasis', Journal of Bone and Mineral Research, 19(3), pp. 429–435.
6.Urakawa, I. et al. (2006) 'FGF23 produces hypophosphatemia by suppressing renal sodium-phosphate cotransporters', Kidney International, 69(4), pp. 543–553.
7.Kuro-o, M. (2009) 'Klotho and aging', Biochimica et Biophysica Acta, 1790(10), pp. 1049–1058.
8.Hu, M.C. et al. (2011) 'Klotho deficiency causes vascular calcification', Journal of the American Society of Nephrology, 22(6), pp. 1245–1253.
9.Faul, C. et al. (2011) 'FGF23 induces left ventricular hypertrophy', Journal of Clinical Investigation, 121(11), pp. 4393–4408.
10.Grabner, A. et al. (2015) 'FGF23/FGFR4-mediated cardiac hypertrophy', Journal of Clinical Investigation, 125(5), pp. 1941–1952.
11.Xie, J. et al. (2014) 'FGF23 and cardiovascular disease in CKD', Nature Reviews Nephrology, 10, pp. 686–699.
12.Gutiérrez, O.M. et al. (2008) 'FGF23 and mortality in CKD', New England Journal of Medicine, 359, pp. 584–592.
13.Saito, T. et al. (2000) 'Cloning and function of Klotho', Nature, 399, pp. 570–574.
14.Hu, M.C. et al. (2015) 'Soluble Klotho and cardioprotection', Kidney International, 88(6), pp. 1270–1278.
15.Vervloet, M.G. & Massy, Z.A. (2012) 'CKD-MBD pathophysiology', Nature Reviews Nephrology, 8, pp. 691–700.
16.Razzaque, M.S. (2009) 'FGF23 and cardiac remodeling', Nature Reviews Nephrology, 5, pp. 649–658.
17.Grabner, A. et al. (2017) 'FGFR4 signaling in the heart', Circulation Research, 120(11), pp. 1830–1844.
18.Richter, M. et al. (2016) 'FGF23-induced cardiac hypertrophy independent of Klotho', Cardiovascular Research, 110(1), pp. 91–101.
19.Shalhoub, V. et al. (2012) 'Anti-FGF23 therapy in CKD models', Journal of Bone and Mineral Research, 27(7), pp. 1510–1517.
20.Shimizu, Y. et al. (2012) 'FGF23 neutralization and phosphate toxicity', Kidney International, 82(10), pp. 1102–1110.
21.Stubbs, J.R. et al. (2007) 'FGF23 excess and cardiovascular risk', Journal of Clinical Endocrinology & Metabolism, 92(11), pp. 4455–4462.
22.Wolf, M. & White, K.E. (2014) 'FGF23 in CKD: pathophysiology and implications', Kidney International, 86(1), pp. 7–9.
23.Ding, Y. et al. (2013) 'Drp1-mediated mitochondrial fission in cardiac injury', Circulation Research, 113(8), pp. 890–902.
24.Ong, S.B. & Hausenloy, D.J. (2010) 'Mitochondrial dynamics in cardiovascular disease', Cardiovascular Research, 88(1), pp. 25–36.
25.Archer, S.L. (2013) 'Mitochondrial dynamics in cardiovascular disease', Circulation Research, 112(8), pp. 1128–1141.
26.Smirnova, E. et al. (2001) 'Drp1 in mitochondrial fission', Journal of Cell Biology, 155(5), pp. 723–734.
27.Hom, J.R. et al. (2007) 'Drp1 phosphorylation regulates mitochondrial division', Journal of Biological Chemistry, 282(17), pp. 12203–12213.
28.Wai, T. & Langer, T. (2016) 'Mitochondrial dynamics and disease', Nature Reviews Molecular Cell Biology, 17, pp. 679–692.
29.Bhandari, S. et al. (2016) 'CKD rat models and cardiovascular outcomes', Nephrology Dialysis Transplantation, 31(10), pp. 1670–1680.
30.Vaziri, N.D. (2004) 'Oxidative stress in CKD', Kidney International, 63(5), pp. 1759–1768.

Vol. 5 No. 2 (2026)

Pakistan Journal of Medical & Cardiological Review

https://pakjmcr.com/index.php/1/about

Online ISSN 3007-2387

Print ISSN 3007-2379